



## Numerical Analysis of Turbulent Fluid Flow and Heat Transfer in a Rectangular Elbow

R. Debnath<sup>1</sup>, A. Mandal<sup>2†</sup>, S. Majumder<sup>3</sup>, S. Bhattacharjee<sup>4</sup> and D. Roy<sup>5</sup>

<sup>1,2,4</sup> Research Scholar, Department of Mechanical Engineering, Jadavpur University, Kolkata-700032, West Bengal, India

<sup>3</sup> Professor, Department of Mechanical Engineering, Jadavpur University, Kolkata-700032, West Bengal, India

<sup>5</sup> Associate Professor, Department of Mechanical Engineering, Jadavpur University, Kolkata-700032, West Bengal, India

†Corresponding Author Email: [arindam.mmeju@gmail.com](mailto:arindam.mmeju@gmail.com)

(Received August 3, 2013; accepted April 7, 2014)

### ABSTRACT

The numerical analysis of turbulent fluid flow and heat transfer through a rectangular elbow has been done by  $\kappa-\varepsilon$  model with standard wall function. Different inlet uniform velocities of 5m/s, 10m/s, 15 m/s, 20 m/s and 25 m/s corresponding to Reynolds numbers of  $Re_1= 4.09 \times 10^4$ ,  $Re_2= 8.17 \times 10^4$ ,  $Re_3= 12.25 \times 10^4$ ,  $Re_4= 16.34 \times 10^4$  and  $Re_5= 20.43 \times 10^4$  have been considered for the numerical experimentations. The fluid considered was incompressible, Newtonian non-reacting and the flow was fully turbulent. The heat transfer analysis has been carried out by considering the fluid having at a higher temperature while the wall kept at lower temperature. A detailed study of the turbulent fluid flow shows that presence of recirculation is inevitable at every corner position or at every bend indicating presence of secondary flow incurring energy losses. The velocity distributions at different stations along the downstream path of the elbow have been plotted. The presence of this adverse pressure gradient is confirmed by the reverse velocity or the negative velocity in the vicinity of the vertical wall. In the upper corner there is a vortex extending from the upper wall of the upper limb almost touching the end point of the left wall of the vertical portion of the elbow. The heat transfer also shows the similar tendency as the fluid flow field influences the convective heat transfer process. The detail temperature distributions across any cross section basically explain the dependence of the convective heat transfer on the fluid flow field.

**Keywords:** Rectangular Elbow, Turbulent Flow, Forced Convection, Recirculation, FLUENT 6.3.

### NOMENCLATURE

$X$	axial coordinate along the duct, m	$L_1$	Length of the bottom limb, m
$Y$	normal coordinate along the duct, m	$L_2$	Length of the upper limb, m
$\bar{u}$	time mean velocity along x axis, m/s	$\mu_l$	Molecular or laminar viscosity, kg/ms
$\bar{v}$	time mean velocity along y direction, m/s	$\mu_t$	Eddy or turbulent viscosity, kg/m s
$u_{in}$	average inlet velocity, m/s	$\mu_{eff}$	Effective Viscosity, kg/m s
$U_b$	Bulk velocity, m/s	$\varepsilon$	Turbulence dissipation rate, $m^2s^{-3}$
$H$	Height of the Elbow, m	$\sigma_k$	prandtl number of the turbulent K. E.
$G$	Rate of Production, $m^2s^{-2}$	$\sigma_\varepsilon$	dissipation energy
$\kappa$	Turbulence kinetic energy, $m^2s^{-2}$	$\rho_{air}$	density of air, $kg/m^3$
$Re$	Reynolds number $(\rho u_{in} D_H) / \mu_l$	$\rho_{al}$	density of Aluminium, $kg/m^3$
$C_\mu$	Empirical Constant	$T_w$	wall Temperature of the Elbow, K
$C_1, C_2$	Empirical constants	$D_H$	hydraulic Diameter of the Elbow, m
$T_i$	Inlet Temperature, K		

### 1. INTRODUCTION

Turbulent fluid flow and heat transfer are familiar phenomena, occurring frequently in many Engineering applications, such as, pipe-flow systems in the

chemical, power plant and petroleum industries, heating, ventilation and air-conditioning (HVAC) ducts around buildings, compact heat exchangers, gas turbine cooling systems, nuclear reactors, harmful air pollutants and dust transportation system, and other many fluidic

devices etc. However, some common characteristics of all turbulent flows are observed as irregularity in time and space, violent mixing, nonlinearity, large Reynolds numbers, sources of noise and dissipation. In forced-convection turbulent flow through a curved duct, the characteristics of the flow field as well as temperature field become more complex than flows in straight duct owing to existence and influence of the secondary flow on the developing flow field and transportation of thermal energy by secondary flow in the duct. Some of the practical applications of the elbow type duct can be specified as ducting system of air pollution control (APC) equipments used in the thermal power plants and many chemical plants, conveying mill duct system and frequently used internal cooling passages of many turbo machinery systems. The analysis of turbulent flow and heat transfer in a stationary bend non-circular duct is of great importance from the engineering viewpoint, and this engineering problem still demands a deeper insight into the physical mechanism of the flow and heat transfer.

Many extensive experimental and numerical studies have been devoted to the forced turbulent flow accompanied by secondary flow through non-circular bend duct to understand the transport mechanism. In earlier studies, several authors such as Launder and Ying, (1972), Gessner, (1973), Launder and Spalding, (1974) and Melling and Whitelaw, (1976) had considered numerous conditions and put effort to highlight their observations to explain the detailed characteristics of turbulent flow fields within the straight and bend ducts of different cross sections, and revealed that the turbulent stress field becomes considerably complex owing to the occurrence of the secondary flow patterns. In other study, the unsteady Navier-Stokes equations were numerically solved by Kim *et al.*, (1987) at a Reynolds number of 3300, based on the mean centerline velocity and channel half-width. Fu *et al.*, (1991) studied the tee configuration including the geometry of rectangular cross-section, but little attention has paid to study the flow conditions in the bifurcation region. The numerical modeling of a turbulent flow in a tee of rectangular cross-section was conducted by Chen *et al.*, (1992) assuming symmetry in the branch exit. Later, Gao and Sundén, (2004) implemented particle image velocimetry (PIV) measurement technique to study air flow characteristics in a rib-roughened rectangular duct at a relatively low Reynolds number of 5800. Hidayat and Rasmuson, (2007) used CFD modeling to describe the drying phenomena occurring in pneumatic conveying drying in the U-bend. Ting *et al.*, (2009) solved Reynolds averaged Navier-Stokes equations by employing 3-D  $k - \omega$  turbulence model to obtain the mean flow characteristics of 90° equal-width open-channel junction. Luo and Razinsky, (2009) studied the turbulent flows through a number of 2D and 3D 180° U-ducts, with and without guide vanes, employing the Reynolds-averaged Navier-Stokes equation. The experimental study of turbulent air flow through rectangular elbow was however carried out by Debnath *et al.*, (2008) at various high blower speeds to explore velocity profiles, flow separation and re-circulation as generated inside the elbow duct. Mandal *et al.* (2010) have analyzed experimentally the turbulent air flow through a

rectangular elbow duct at two low blower speeds only. Recently, Bhattacharjee *et al.* (2011) have conducted an investigation to study the behavior of turbulent air flow through a two-dimensional rectangular diffuser using the same experimental apparatus with forced convection turbulent duct flow, to understand the transport mechanism in bend ducts of different cross-sections. Investigation by experimental and numerical methods been done for past few decades, and a detailed survey of the relevant literatures is hereby given in this paper. Aissa *et al.*, (2013) investigated a curved 90° square bend in an open-circuit horizontal-to-horizontal suction wind tunnel system. They used sand particle to represent the solid phase with a wide range of particle diameters. Brundrett and Burroughs, (1967) presented experimentally the distributions of mean temperature in a vertical square duct and revealed that the influences of the secondary flow appears in the local wall heat-flux distributions. Johnson and Launder, (1985) measured local heat transfer coefficients and temperature distributions within the fluid for air flow in a range of Reynolds numbers from  $9.9 \times 10^3$  to  $9.2 \times 10^4$  around an 180° square-sectioned bend duct. By using numerical methods, Launder and Ying, (1973), Emery *et al.*, (1980), Nakayama and Koyama, (1986), Launder, (1988), Rokni and Sundén, (1996), Campo *et al.*, (1996) and Valencia, (2000) obtained the velocity fields and temperature distributions in the duct assuming negligible eddy-diffusivities and constant Prandtl number over the duct cross section. In the study of Wang *et al.*, (2001), both experimental and numerical approaches were adopted to investigate the fluid flow and heat transfer characteristics of air in the developing region for twisted square ducts with constant or varying cross section. The elliptic relaxation turbulence model  $\sqrt{\nu^2} - f$  has been applied by Mehdizadeh *et al.* in (2008) to simulate the motion of turbid density currents laden with fine solid particle. Recently, the computational study of Razak *et al.*, (2009) has comprehensively simulated the use of  $k-\epsilon$  model for predicting flow velocity and temperature field distributions in 180° sharp bend region of the multiple rectangular ducts. Debnath *et al.*, (2009), investigated re-circulations generated due to jet inlet flow estimating the sizes and strength of re-circulation bubbles formed in the bent portions of the rectangular elbow duct. Debnath *et al.*, (2010) also presented a comparative study between three types of turbulent models i.e. standard  $k-\epsilon$ ,  $k-\omega$  and Reynolds stress models with flow visualization for the turbulent air flow in a two-dimensional rectangular elbow. Khaleghi *et al.* (2010) used four common turbulence models other than standard  $k-\epsilon$  model to simulate transient flow in a pipe at Reynolds number (based on bulk velocity and diameter) ranged from 7000 to 45200. Sutardi *et al.* (2010) investigates the flow phenomenon in a 90° elbow to examine the effect of insertion of guide vane on pressure loss. In the numerical work of Shirani *et al.* (2011) the turbulent interfacial flow was studied using LES and RANS equations for modeling and simulation of 2D and 3D in compression time dependent Navier-Stokes equations for a two fluid problem. Theoretical and experimental investigations of the flow of air through a square section duct with installed bend were done by Rup and Sarna (2011). Ono *et al.* (2011)

investigate the influence of elbow curvature on flow structure at elbow outlet under high Reynolds number condition.

The present study is concerned with two-dimensional analysis of the turbulent fluid flow and forced convection heat transfer in an elbow duct of rectangular cross-section with uniform wall temperature condition and different inlet uniform velocities of fluid flow. The present authors are inspired to investigate such a complicated flow owing to the fact that such a flow along with heat transfer is challenging particularly in the perspective of turbulent fluid flow and heat transfer. It is common to lot of industrial applications and generation of recirculation regions with low pressure zone influencing the heat transfer etc. The inlet temperature is also uniform and greater than the wall temperature. The aim is to gain improved understanding of turbulent fluid flow and thermal characteristics by analyzing the velocity as well as temperature distribution curves at different stations along the downstream path of the elbow. Numerical results are reported for incompressible, Newtonian turbulent air flow entering the stationary rectangular duct with uniform velocity and temperature profiles across the entrance section and under uniform wall temperature condition. Numerical Control Volume Formulation method using CFD program software Fluent 6.2 © Fluent Inc. 2004 is applied in this investigation work.

## 2. GEOMETRICAL DESCRIPTION

The experimental geometry is two-dimensional rectangular elbow with lengths  $L_1 = 0.810$  m,  $L_2 = 0.660$  m, height,  $H = 0.33$  m and width  $W = 0.135$  m as illustrated in Fig.1a. The air is admitted through inlet of the duct at a prescribed uniform speed and at a temperature greater than walls temperature of the duct. In this case, the walls are kept hot at a constant temperature as shown in Fig.1a. The air flow throughout the duct is turbulent and hydro-dynamically fully developed at the exit. The total length is divided into three parts as shown in the Fig.1b.

## 3. NUMERICAL MODEL AND SOLUTION

The mass and momentum conservation equations in two dimensional Cartesian coordinate system for the turbulent mean flow with eddy viscosity models are given as follows:

### 3.1 Continuity Equation

$$\frac{\partial(\rho\bar{u})}{\partial x} + \frac{\partial(\rho\bar{v})}{\partial y} = 0 \quad (1)$$

### 3.2 Momentum Equation

- X- Component

$$\rho \left[ u \frac{\partial \bar{u}}{\partial x} + v \frac{\partial \bar{u}}{\partial y} \right] = -\frac{\partial p}{\partial x} + 2 \frac{\partial}{\partial x} \left( \mu_{eff} \frac{\partial \bar{u}}{\partial x} \right) + \frac{\partial}{\partial y} \left\{ \mu_{eff} \left( \frac{\partial \bar{u}}{\partial y} + \frac{\partial \bar{v}}{\partial x} \right) \right\} \quad (2)$$

$$\frac{\partial}{\partial y} \left\{ \mu_{eff} \left( \frac{\partial \bar{u}}{\partial y} + \frac{\partial \bar{v}}{\partial x} \right) \right\}$$

- Y- Component

$$\rho \left[ u \frac{\partial \bar{v}}{\partial x} + v \frac{\partial \bar{v}}{\partial y} \right] = -\frac{\partial p}{\partial y} + 2 \frac{\partial}{\partial y} \left( \mu_{eff} \frac{\partial \bar{v}}{\partial y} \right) + \frac{\partial}{\partial x} \left\{ \mu_{eff} \left( \frac{\partial \bar{u}}{\partial x} + \frac{\partial \bar{v}}{\partial y} \right) \right\} \quad (3)$$

## 3.3 Energy Equation

The temperature distribution of the fluid is described by the energy equation in two dimensional Cartesian coordinate systems.

$$\rho \left[ \frac{\partial(\bar{uT})}{\partial x} + \frac{\partial(\bar{vT})}{\partial y} \right] = \frac{\partial}{\partial x} \left[ \left( \frac{\mu_l}{Pr} + \frac{\mu_t}{\sigma_T} \right) \frac{\partial T}{\partial x} \right] + \frac{\partial}{\partial y} \left[ \left( \frac{\mu_l}{Pr} + \frac{\mu_t}{\sigma_T} \right) \frac{\partial T}{\partial y} \right] \quad (4)$$

The effective viscosity is given by,

$$\mu_{eff} = \mu_l + \mu_t \quad (5)$$

Where  $\mu_l$  and  $\mu_t$  are laminar and eddy viscosity respectively.

The eddy viscosity is given by

$$\mu_t = \frac{\rho C \mu k^2}{\varepsilon} \quad (6)$$

## 3.4 Standard $k-\varepsilon$ turbulent model Equation

- $k$  - Equation

$$\rho \left[ u \frac{\partial k}{\partial x} + v \frac{\partial k}{\partial y} \right] = \frac{\partial}{\partial x} \left[ \left( \mu_l + \frac{\mu_t}{\sigma_k} \right) \frac{\partial k}{\partial x} \right] + \frac{\partial}{\partial y} \left[ \left( \mu_l + \frac{\mu_t}{\sigma_k} \right) \frac{\partial k}{\partial y} \right] + G - \rho \varepsilon \quad (7)$$

- $\varepsilon$  - Equation

$$\rho \left[ u \frac{\partial \varepsilon}{\partial x} + v \frac{\partial \varepsilon}{\partial y} \right] = \frac{\partial}{\partial x} \left[ \left( \mu_l + \frac{\mu_t}{\sigma_k} \right) \frac{\partial \varepsilon}{\partial x} \right] + \frac{\partial}{\partial y} \left[ \left( \mu_l + \frac{\mu_t}{\sigma_k} \right) \frac{\partial \varepsilon}{\partial y} \right] + C_1 \frac{\varepsilon}{k} G - C_2 \rho \frac{\varepsilon^2}{k} \quad (8)$$

Here,  $C_1, C_2, \sigma_k$  and  $\sigma_\varepsilon$  are the empirical turbulence constants, and some typical values of these constants in the standard  $k-\varepsilon$  model are recommended by Launder and Spalding [1974] which are given below-

$C_1$	$C_2$	$\sigma_k$	$\sigma_\varepsilon$	$C_\mu$
1.44	1.92	1.0	1.3	0.09

$$G = \mu_t \left[ 2 \left\{ \left( \frac{\partial \bar{u}}{\partial x} \right)^2 + \left( \frac{\partial \bar{v}}{\partial y} \right)^2 \right\} + \left( \frac{\partial \bar{u}}{\partial y} + \frac{\partial \bar{v}}{\partial x} \right)^2 \right] \quad (9)$$

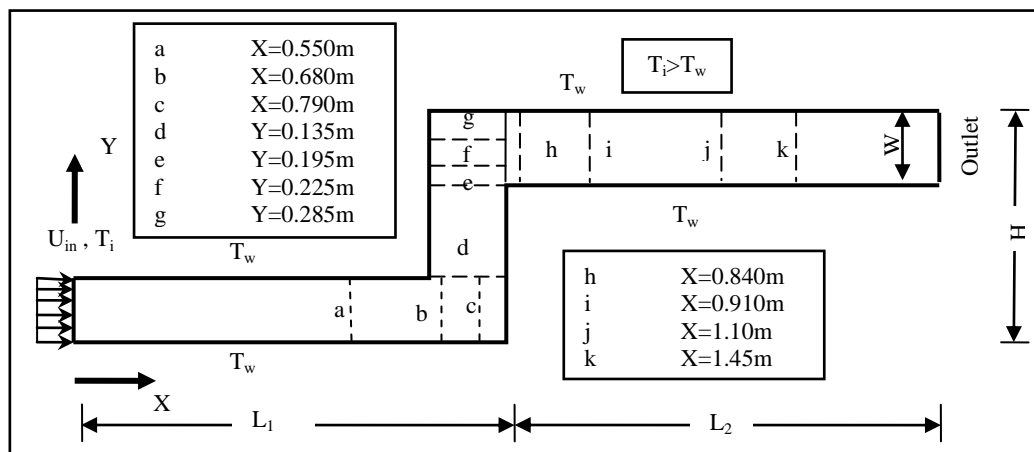


Fig. 1a. Schematic view of Elbow duct

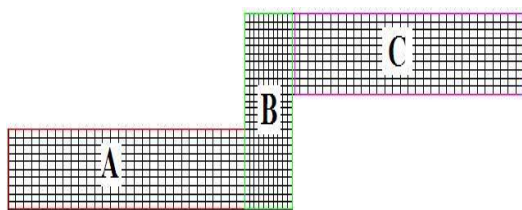


Fig. 1b. Typical Grid structure for numerical experimentation

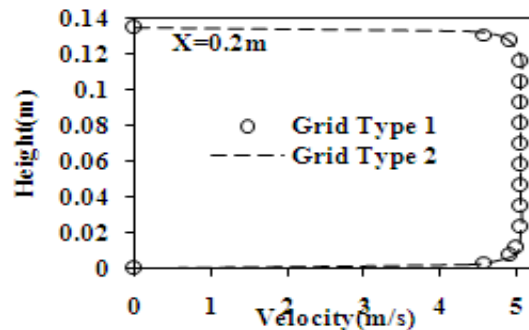


Fig. 1c. Grid Independent study

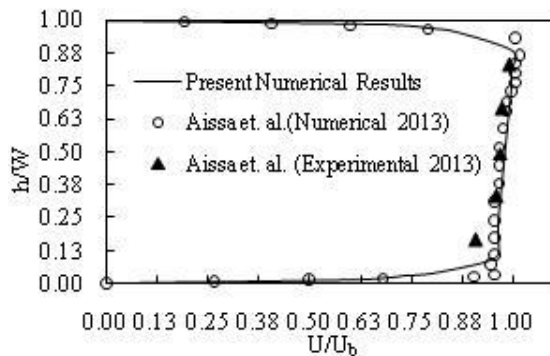


Fig. 1d. Validation of the Present Work

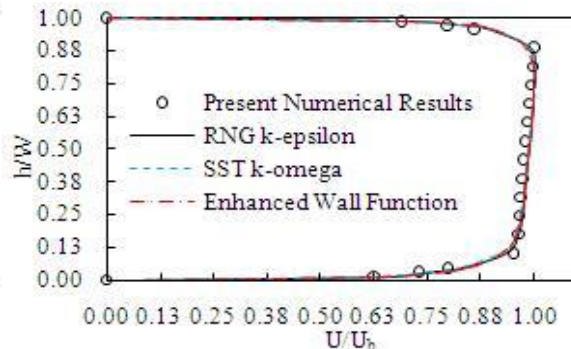


Fig. 1e. Comparison of results of different Turbulence Models

The standard wall function has been adopted from their derivations for the solution of the  $k-\epsilon$  equations for the problem investigated here.  $G$  corresponds to the turbulent shear production rate.

### 3.5 Boundary Conditions

For present analysis the working fluid is air at 350K with density taken as  $\rho_{air} = 1.132 \text{ kg/m}^3$ , viscosity,  $\mu_i = 1.87 \times 10^{-5} \text{ Kg/m-s}$

#### At the Inlet:

The inlet axial velocity is uniform.

$u_m$  Varies from 5 m/s to 25 m/s, at an interval of 5 m/s  
 $T_i = 350\text{K}$ , Inlet Temperature

#### At the Wall:

No slip condition has been taken for velocities so  $u = v = 0$   
 $T_w = 300\text{K}$ , Wall Temperature

#### At the Outlet:

Fully developed flow condition has been taken at the outlet.

$$\frac{\partial \phi}{\partial x} = 0, \phi \text{ stands for } u, v, \kappa, \epsilon, T$$

The geometry of the numerical model consists of an

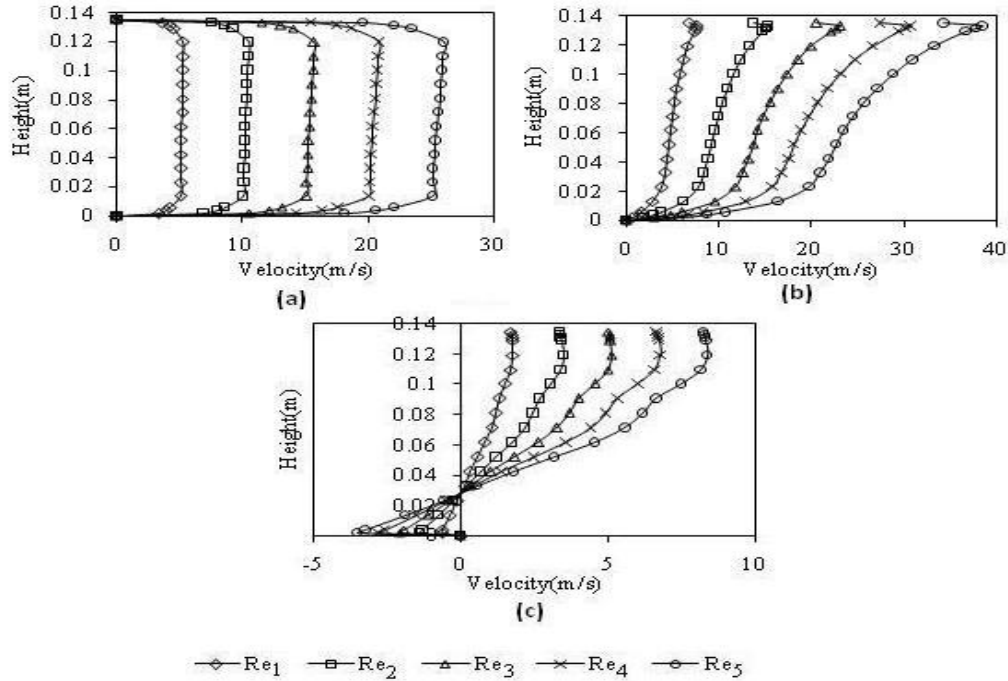


**Fig. 2. Velocity profile in the lower Limb at (a) X=0.550 m, at (b) X=0.680 m, at (c) X=0.790 m**

the fluid is supplied through the duct at velocity 5 m/s, 10 m/s, 15 m/s, 20 m/s, 25 m/s and inlet fluid and wall temperature at 350K and 300K respectively. The working fluid is air of density  $\rho_{air} = 1.132 \text{ kg/m}^3$  and viscosity  $\mu = 1.87 \times 10^{-5} \text{ kg/m-s}$ . The duct material is considered aluminium metal of thickness 0.002 m, density  $\rho_{Al} = 2719 \text{ kg/m}^3$  and thermal conductivity  $k = 202.4 \text{ W/m-K}$  respectively.

Based on the geometrical model, a mesh-model along with grid points is generated in preprocessor tool GAMBIT 2.3 of Fluent Inc., the solution domain is then prepared, compiled and finally solved using the compiler-cum-solver FLUENT 6.3. The CONTROL VOLUME method has been selected to solve the governing equations in 2-D Cartesian co-ordinate system. The *SIMPLER* algorithm of Patankar (1981) is also applied to the pressure-velocity coupling to discretize and solve the turbulent momentum,  $k - \epsilon$  and energy equations under Power Law Scheme. The solution for all the numerical experimentations has been carried out for a uniform mesh-grid system of  $170 \times 70$  mesh for part 'A',  $35 \times 170$  mesh for part 'B' and  $160 \times 70$  mesh part 'C' respectively as shown in Fig.1. The numerical solution is assumed to get converged when the absolute residual values of (i) Continuity, Momentum, Turbulent  $k - \epsilon$  and (ii) Energy for 1000 iteration cycles are less than 0.0001. The convergence criterion ensures that area weighted average wall  $Y^+$  value is checked fifty or less. The numerical solution is also assumed to become converged when the net residual value of the total heat transfer rates for successive iteration cycles is less than 0.01%.

#### 4. RESULTS AND DISCUSSION

elbow duct with rectangular cross section. In this case,

The turbulent air flow with forced convective heat transfer has been considered to be entered with different uniform velocities through the inlet of the lower horizontal limb of the two-dimensional rectangular elbow having a prescribed uniform wall temperature. The turbulent flow along with temperature field is investigated numerically and the results are plotted for the different locations along X-Y-X directions.

In the Fig.1b a typical grid system has been shown, while in the Fig.1c a grid independent study has been shown. Type 1 grid system is zone A( $100 \times 35$ ), B( $35 \times 100$ ) and C( $100 \times 35$ ), while type 2 indicates A( $100 \times 50$ ), B( $50 \times 120$ ) and C( $100 \times 50$ ) grid systems. The matching has been observed very much satisfactory. It is therefore stated that all the numerical works have been carried out with the Type 1 grid system throughout this paper. In Fig. 1d the numerical result is compared with the experimental results of Aissa *et al.* (2013). The close matching confirms that the present method is very much accurate. The percentage of relative error is 0.01%. From the Fig. 1e, it has been observed that the results are almost same for different turbulence models. That is the justification for using standard  $k - \epsilon$  model for the sake of simplicity.

In the Fig. 2(a), (b) and (c) The Reynolds Numbers  $Re_1, Re_2, Re_3, Re_4$  and  $Re_5$  represents the corresponding Reynolds number of  $4.09 \times 10^4, 8.17 \times 10^4, 12.25 \times 10^4, 16.34 \times 10^4$  and  $20.43 \times 10^4$  respectively. In the present work unless otherwise stated all the Reynolds numbers used are the same as these. In the Fig. 2(a), five mean velocity profiles are obtained at a station distance  $X=0.550 \text{ m}$  for five different turbulent Reynolds numbers of air flow at inlet while in Fig. 2(b) and 2(c), the velocity profiles clearly depict that the

recirculation begins and continues to grow at station distances  $X=0.680$  m and  $X=0.790$  m respectively along the lower horizontal limb part. Figure 3 confirms

generation of recirculation flow in the corner zone of

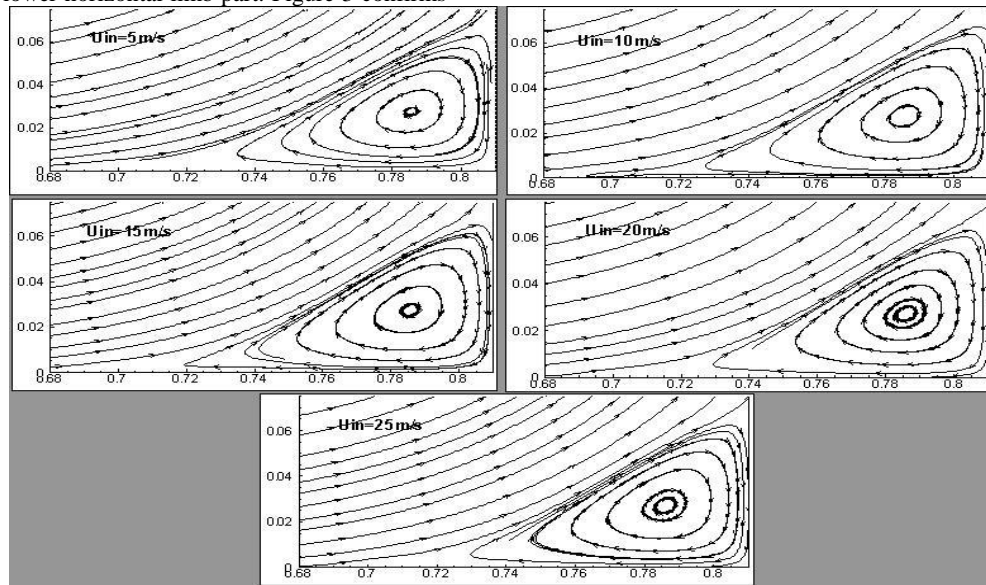


Fig. 3. Vortex formation in the lower Limb (Vortex1)

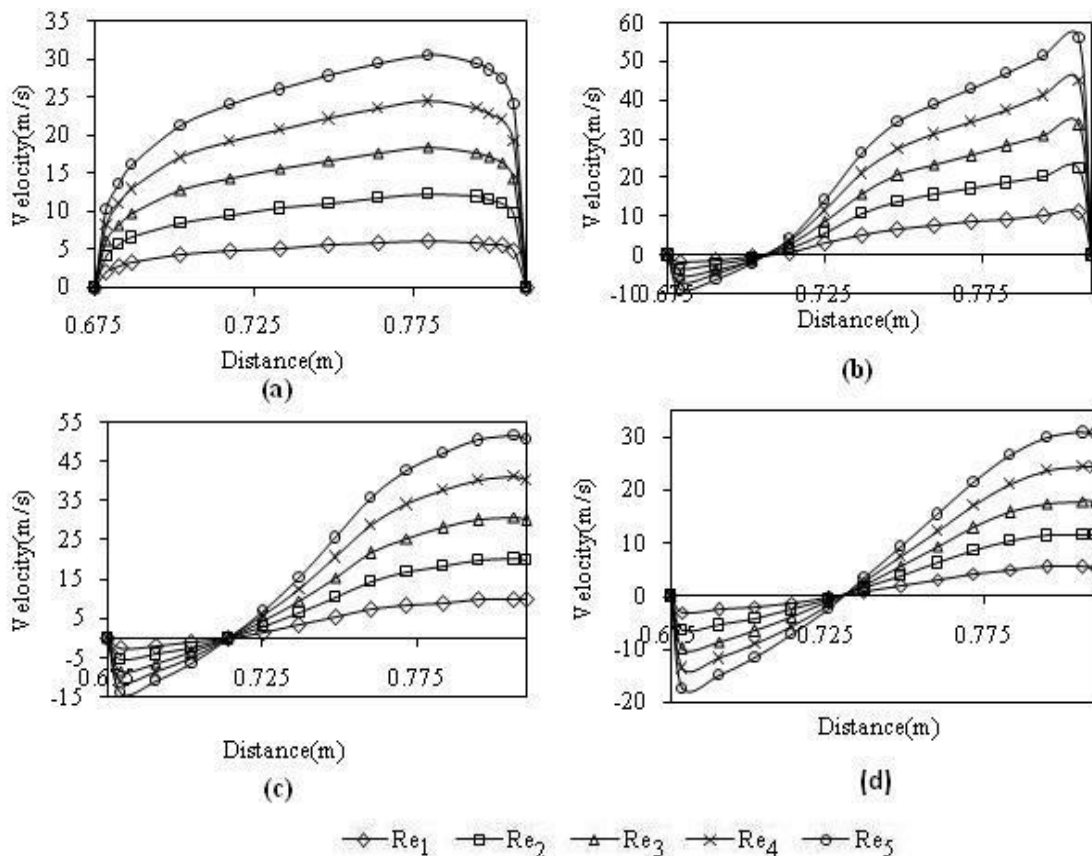


Fig. 4. Velocity profile in the vertical limb at (a)  $Y=0.135$ m, (b)  $Y=0.195$ m, (c) at  $Y=0.225$ m, (d) at  $Y=0.285$ m

the limbs A and B at different inlet velocities of air flow. In the similar way, five uniform velocity profiles are obtained at a distance  $Y=0.135$ m in the vertical limb B as shown in Fig. 4(a). Similarly Fig. 4(b) to 4(d) clearly depict the existence of recirculation at distances

$Y=0.195$ m,  $Y=0.225$  m and  $Y=0.285$ m respectively. Fig. 5 illustrates the recirculation generated in the corner zone in between the limbs B and C at different inlet velocities of air flow.

In the Fig. 6(a) and 6(b), the occurrence of recirculation still exists at distances of  $X=0.840$  m and  $X=0.910$  m inside the upper limb C and the figures 6(c) and 6(d) show the reattachment of the turbulent flow at the

downstream of the elbow. Fig. 7 gives the views of

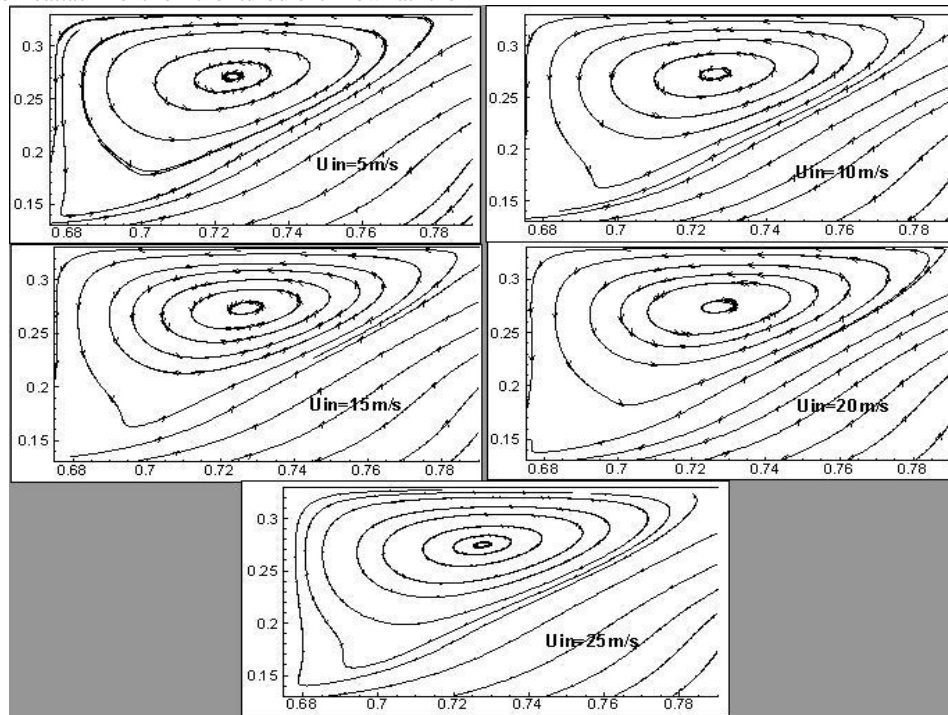


Fig. 5. Vortex formation of vertical limb (Vortex 2)

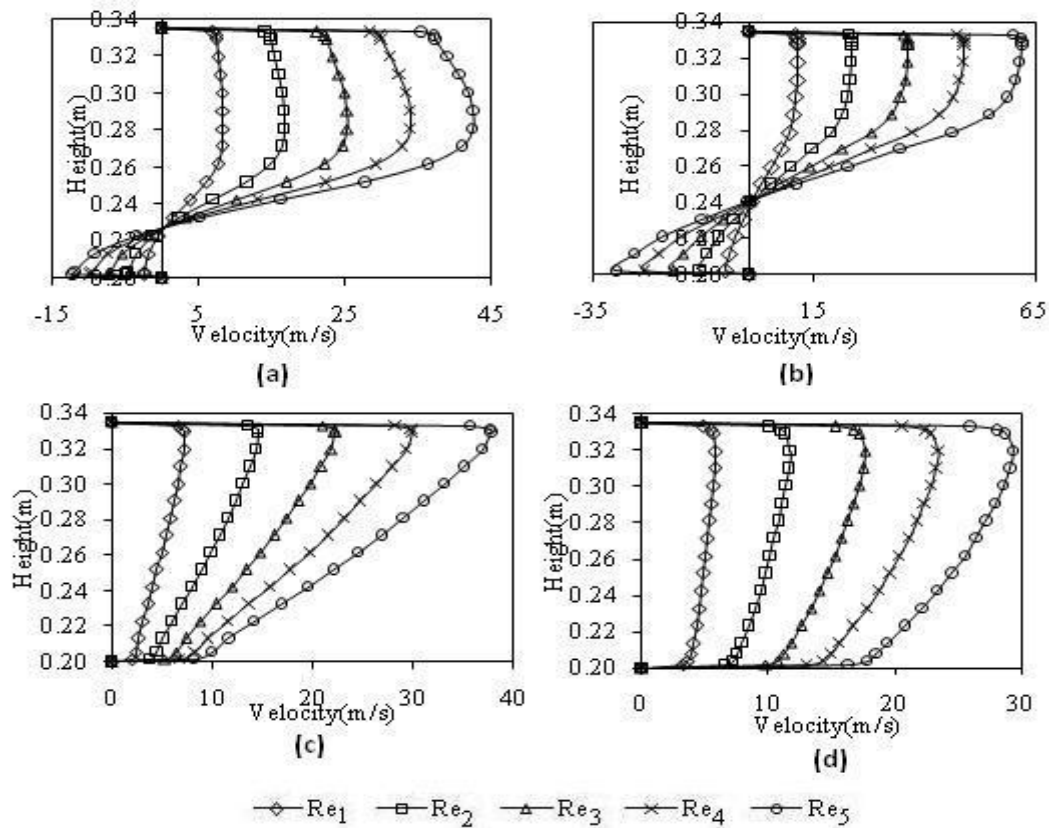
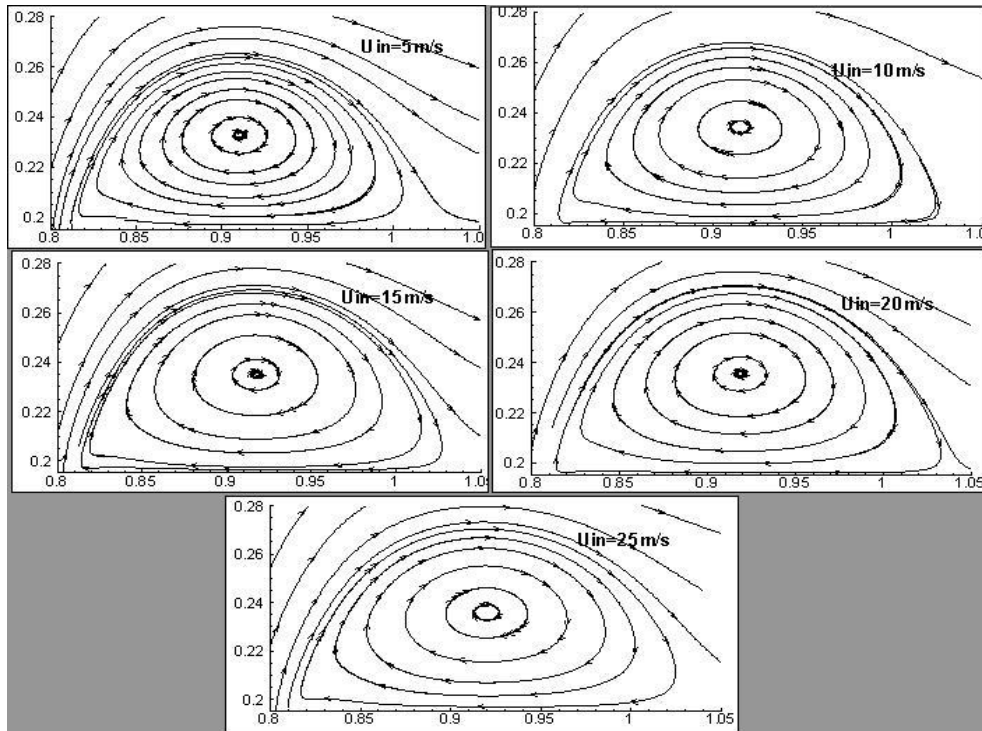
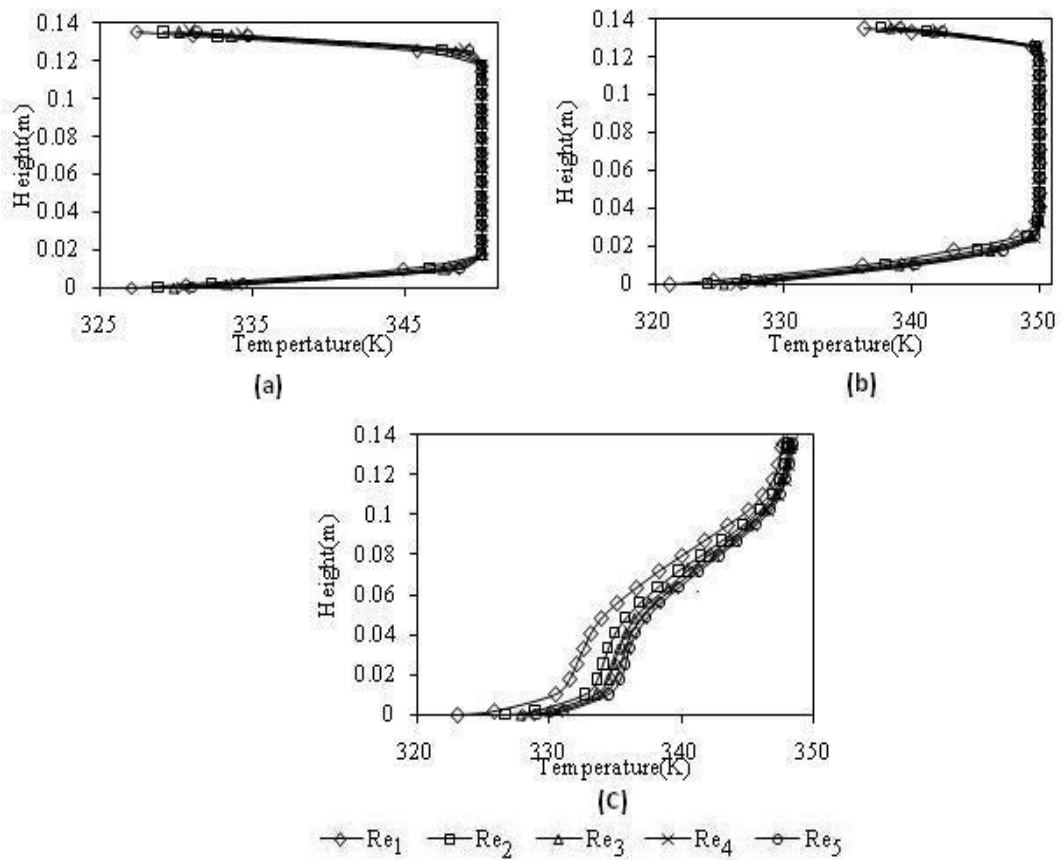


Fig. 6. Velocity profile in the upper limb at (a)  $X=0.84$ m, (b)  $X=0.91$ m, (c)  $X=1.1$ m, (d)  $X=1.45$ m



**Fig. 7. Vortex formation of upper limb (Vortex 3)**



**Fig. 8. Temperature profile of Lower Limb at (a)  $x=0.55\text{m}$ , (b)  $X=0.68\text{m}$ , (c)  $X=0.79\text{m}$**



vortex formation at a location nearer to lower bend inside the upper horizontal limb of the elbow.

In the Fig. 8(a) to 8(c), temperature distributions for five different turbulent Reynolds numbers and at different heights and distances inside the lower horizontal limb have been illustrated. The temperature profiles obtained are almost constant irrespective of the height and Reynolds numbers at distances  $X=0.55$  m and  $X=0.68$  m respectively whereas it gradually increases with increasing value of turbulent Reynolds numbers as well as heights at a station distance  $X=0.79$  m.

Fig. 9 shows good results of the gradual increment of temperature distributions with respect to the increasing value of Reynolds numbers of the turbulent air flow through the vertical limb of the elbow.

Similarly, no remarkable change in temperature distributions has been observed at the downstream part of the elbow as shown in Fig. 10.

However there has been a difference in the temperature profiles as shown in the Fig. 10a and 10b. This is due to the effect of the recirculation bubble present at that region.

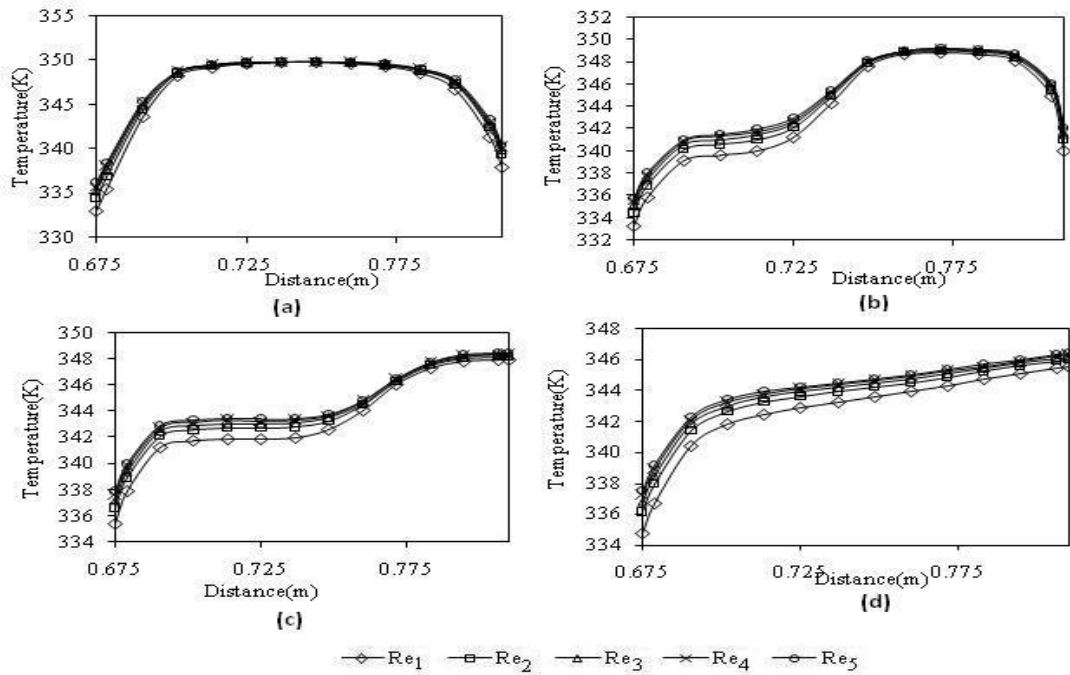


Fig. 9, Temperature profile of vertical limb at (a)  $Y=0.135$ m, (b)  $Y=0.195$ m, (c)  $Y=0.255$ m, (d)  $Y=0.315$ m

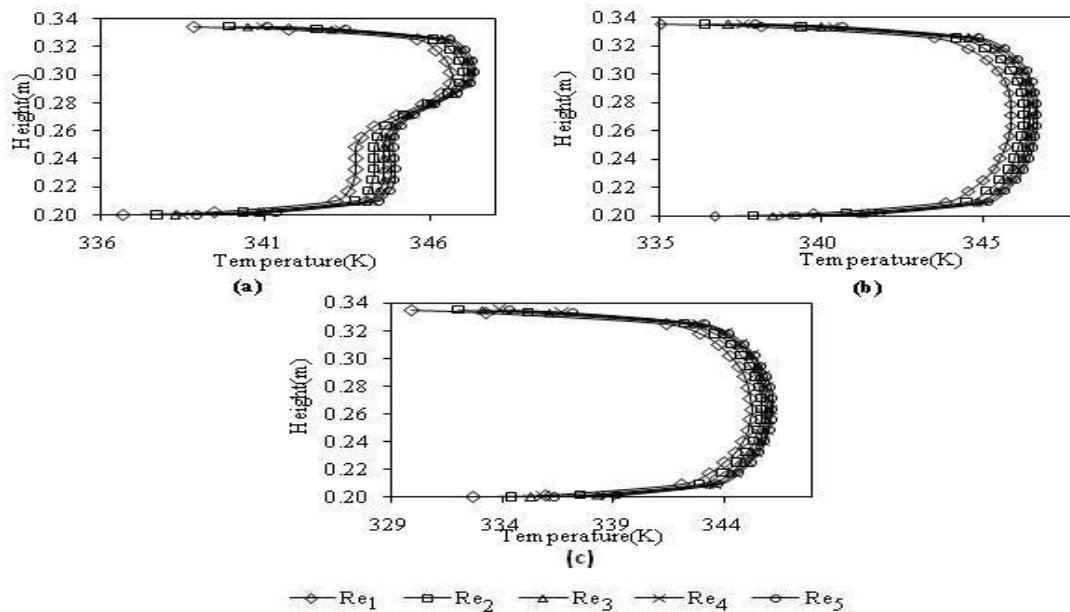


Fig. 10. Temperature profile of the upper limb at (a)  $X=0.91$ m, (b)  $X=1.1$ m, (c)  $X=1.45$ m

## 5. CONCLUSION

A numerical experimentation of a conjugate heat and developing fluid flow in a rectangular elbow has been done. The Following are the conclusions:-

- There has been generation of recirculation at different bend positions. However the recirculation strengths have been observed to be stronger at the upper limb of the duct.
- The secondary flow of recirculation strongly influences the main stream flow as well as the heat transfer phenomena.
- It is also observed that the turbulent convection flow is likely to become fully developed in downstream part of the elbow. However more extensive studies are needed for fully exploring the complicated flow and heat transfer by convective methods as it is indicated in the present study.

## ACKNOWLEDGEMENTS

The authors express their sincere thanks and gratitude to all who are extending their helping hand by giving valuable suggestions and technical support for this work done at Hydraulics Laboratory, Mechanical Engineering Department, Jadavpur University, Kolkata (India).

## REFERENCES

- Aissa, W. A., Mekhail, T. A. M., Hassanein, S. A., and Hamdy, O. (2013). Experimental and Numerical Study of Dilute Gas-Solid Flow inside a 90° Horizontal Square Pipe Bend. *Open journal of fluid dynamics*, 3, 331-339.
- Bhattacharjee, S. Debnath, R. Roy, D. and Majumder, S. (2011). An Experimental Study on Turbulent Air Flow through a Two Dimensional Rectangular Diffuser. *J. IEI Mech Engg*, 92, 3-7.
- Brundrett, E. and Burroughs, P. R. (1967). The temperature inner-law and heat transfer for turbulent flow in a vertical square duct. *Int. J. Heat Mass Trans*, 10, 1133-1142.
- Campo, A. Tebeest, K. Lacoa, U. and Morales, J. C. (1996). Application of a finite volume based method of lines to turbulent forced convection in circular tubes. *Numerical Heat Transfer Part-A Applications*, 30(5), 503-517.
- Chen, H. and Liang, G. (1992). Numerical computation of turbulent flow in T-shape junction. *J. Hydrodynamics*, 4(3), 50-58.
- Debnath, R., Bhattacharjee, S., Roy, D. and Majumder, S. (2008). Experimental Analysis of the Turbulent Fluid Flow through a Two Dimensional Rectangular Elbow. *Proc 53 rd Congress, ISTAM (An Int. meet)*, Osmania Univ., Hyderabad, India, Dec. 27-30, pp. 184-190.
- Debnath, R., Roy, D. and Majumder, S. (2009). Numerical Analysis of the confined central and annular jet flow through a two dimensional elbow. *Conf. Proceedings, CAMSCM 2009, NERIST, India*, pp.209-219.
- Debnath, R. Bhattacharjee, S. Mandal, A. Roy, D. and Majumder, S. (2010). A comparative study with flow visualization of turbulent fluid flow in an Elbow. *IJEST*, 2(9) 4108-4121.
- Emery, A. F., Neighbors, P. K. and Gessner, F. B. (1980). The numerical prediction of developing turbulent flow and heat transfer in a square duct, *J Heat Trans*, 102, 51-57.
- Fu, H., Watkins, A. P., Tindal, M. J. and Yianneskis, M. (1991). Turbulent dividing flow in a branched duct, *ASME Fluids Engg. Conf*, pp. 33-43.
- Gao, X. and Sundén, B. (2004). PIV measurement of the flow field in rectangular ducts with 600 parallel, crossed and V-shaped ribs. *Exp Therm and Fluid Sci*. 28, 639-653.
- Gessner, F. B. (1973). The Origin of Secondary Flow in Turbulent Flow along a Corner. *J Fluid Mech*. 58, 1-25.
- Hidayat, M. and Rasmuson, A. (2007). Heat and Mass Transfer in U-bend of a pneumatic conveying dryer. *Trans, IChemE Part-A*. 85(A3) 307-319.
- Humphrey, J.A.C., Whitelaw, J.H. and Yee, G. (1981). Turbulent flow in a square duct with strong curvature. *J. Fluid Mech*. 103, 443-463.
- Johnson, R. W. and Launder, B. R. (1985). Local Nusselt number and temperature field in turbulent flow through a heated square-sectioned U bend. *Int. J. Heat and Fluid Flow*. 6( 3), 171-180.
- Khaleghi, A., Pasandideh-Fard, M., Malek-Jafarian, M, and Chung, Y. M. (2010). Assessment of Common Turbulence Models under Conditions of Temporal Acceleration in a Pipe. *Journal of Applied Fluid Mechanics*. 3(1), 25-33.
- Kim, J., Moin, P. and Moser, R. (1987). Turbulence statistics in fully developed channel flow at low Reynolds number. *J Fluid Mech*. 177, 137-166.
- Kim, K., Wiedner, B. G. and Camci, C. (2002). Turbulent Flow and Endwall Heat Transfer Analysis in a 90° Turning Duct and Comparisons with Measured Data. *Int. J. Rotating Machinery*. 8(2), 109-123.
- Launder, B. E. (1988). On the computation of convective heat transfer in complex turbulent flows. *J Heat Trans*. 110, 1112-1228.
- Launder, B. E. and Ying, W. M. (1972). Secondary Flows in Ducts of Square Cross-section. *J Fluid Mech*, 54, 289-295.
- Launder, B. E. and Ying, W. M. (1973). Prediction of flow and heat transfer in ducts of square cross-section. *Proc Inst Mech Engg*. 187, 455-461.

- Launder, B. E. and Spalding, D. B. (1974). The Numerical Computation of Turbulent Flows. *Comp Meth Appl Mech Engg.* 3(2), 269-289.
- Luo, J. and Razinsky, E. H. (2009). Analysis of Turbulent flow in 180-degree turning ducts with and without guide vanes. *Trans. ASME J Turbo machinery.* 131, 021011-1-10.
- Lu, T., Liu, S.M. and Attinger, D. (2013). Large-eddy simulations of structure effects of an upstream elbow main pipe on hot and cold fluids mixing in a vertical tee junction. *Annals of Nuclear Energy.* 60, 420-431.
- Mandal, A., Bhattacharjee, S., Debnath, R. Roy, D. and Majumder, S. (2010). Experimental Investigation of Turbulent Fluid flow through a Rectangular Elbow. *Int J Engg Sci and Tech.* 2(6), 1500-1506.
- Mehdizadeh, A., Firoozabodi, B. and Farhanieh, B. (2008). Numerical simulation of Turbidity Current using  $\sqrt{2-f}$  Turbulence Model. *Journal of Applied Fluid Mechanics.* 1(2), 45-55.
- Melling, A. and Whitelaw, J. H. (1976). Turbulent flow in rectangular duct. *J Fluid Mech.* 78, 289-315.
- Nakayama, A. and Koyama, H. (1986). Numerical prediction of turbulent flow and heat transfer within ducts of cross-shaped cross section. *J. Heat Trans* 108, 841-847.
- Ono, A., Kimura, N., Kamide, H. and Tobita, A. (2011). Influence of elbow curvature on flow structure at elbow outlet under high Reynolds number condition. *Nuclear Engineering and Design.* 241, 4409-4419.
- Patankar, S. V. (1981). Numerical Heat transfer and fluid flow. *McGraw Hill*, New York.
- Razak, A. A., Yaakob, Y. and Ramli, M. N. (2009). Computational Simulation of turbulence Heat Transfer in Multiple Rectangular Ducts. *World Academy of Science Engineering and Technology,* 53, 242-246.
- Rokni, M. and Sundén, B. (1996). Numerical investigation of turbulent forced convection in ducts with rectangular and trapezoidal cross section area by using different turbulence models, *Numerical Heat Transfer Part A Applications.* 30(4), 321-346.
- Rudolf, P. and Desova, M. (2007). Flow Characteristics of curved ducts. *Applied and Computational Mechanics.* 1, 255-264.
- Rup, K. and Sarna, P. (2011). Analysis of turbulent flow through a square-sectioned duct with installed 90-degree elbow. *Flow Measurement and Instrumentation.* 22, 383-391.
- Sutardi, Wawan, A. W., Nadia, N. and Puspita, K. (2010). Numerical and Experimental Study on the Effect of Guide Vane Insertion on the Flow Characteristics in a 90° Rectangular Elbow. *ICCHT2010 - 5th International Conference on Cooling and Heating Technologies. Bandung, Indonesia 9- 11 December.*
- Ting, Z., Wei-lin, X. and Chao, W. U. (2009). Effect of discharge ratio on flow characteristics in 900 equal-width open-channel junction. *J Hydrodynamics,* 21(4) 541-549.
- Valencia, A. (2000). Turbulent flow and heat transfer in a channel with a square bar detached from the wall. *Numerical Heat Transfer Part-A Applications.* 37(3), 289-306.
- Wang, L. B., Tao W. Q., Wang, W. Q. and He, Y. L. (2001). Experimental and Numerical study of turbulent heat transfer in twisted square ducts, *Trans ASME J Heat Trans.* 123, 868-877.